

LARGE DEFORMATION ANALYSIS OF GROUND WITH WALL MOVEMENT OR SHALLOW FOUNDATION UNDER EXTREMELY LOW CONFINING PRESSURE USING PIV

K. SATO*, H. AKAGI*, T. KIRIYAMA† AND K. ESAKI*

* Department of Civil and Environmental Engineering
Waseda University

58-205, 3-4-1, Ohkubo, Shinjuku-ku, Tokyo, 169-8555, Japan

e-mail :adjl@fuji.waseda.jp, web page : https://www.f.waseda.jp/akagi/index_e.html

† Institute of Technology

Shimizu Corporation

3-4-17, Etchujima, Koto-ku, Tokyo, 135-0044, Japan

e-mail :kiriyaama@shimz.co.jp, web page : <https://www.shimz.co.jp>

Key words: Particle Image Velocimetry (PIV), laminated aluminum bars, wall movement, shallow foundation

Abstract. Large-scale natural disasters have occurred frequently in recent years. In such disasters, large ground deformation has been a recurring phenomenon. As it directly affects the structure, has durable design is necessitated to minimize the damages. Additionally, the fracture process zones are predicted using numerical analysis, and thereafter, the results of the analysis are validated after comparison with the experimental ones. In this study, image analysis is performed using particle image velocimetry (PIV), and subsequently, the analysis results are validated by the comparison. We herein aim to improve the precision of the image-analysis results, and examine the experimental or analytical condition of reproducing the deformation .

1 INTRODUCTION

In the recent years, there are growing concerns about geohazards triggered by earthquakes and heavy rainfalls in Japan. Geohazards, such as slope failure and landslide, have caused heavy damages to social infrastructures. Taking an example of the 2016 Kumamoto Earthquakes, which occurred on 16th April 2016, slope failures, landslides and debris flow occurred mainly around the Mt. Aso area. In particular, large-scale (deep) landslides occurred in Minami-Aso village Tateno area, and Aso Bridge collapsed completely by this slope failure. In order to minimize the risk of such damages, it is desirable to understand the ground collapse process, scale and range. However, large deformation problem of ground that ranges more than tens of meters has mainly been based on case studies such as literature surveys and ground surveys. Along with these investigations, it is necessary to simulate the destruction process by numerical analysis, and the analysis should be evaluated by practical engineering or physical evaluation.

In order to validate the numerical method, the tracking of the deformation of laboratory test results is performed. A deformation measurement method based on Particle Image Velocimetry (PIV) has been used for a tool to geotechnical testing. In the paper, the deformation of ground model with laminated aluminium bars is analyzed with the PIV method. Applying the PIV

method to the model tests, the distribution of displacement can be obtained with higher resolution than that of the method using target markers.

By using PIV, accurate results of deformation analysis in model test, that manages the bearing capacity of shallow footing or deformation analysis on retaining wall movement tests, can be obtained. Also comparing the result of PIV with the numerical analysis, the validity of numerical analysis about large deformation problem is evaluated from shear strain and load settlement relationship in the ground. Through the examination and comparison of the results of both model test analysis and numerical analysis, the study aims to the approximation of reproducing the actual phenomena based on numerical analysis such as DEM, FEM or other methods.

2 DEFORMATION ANALYSIS OF MODEL TESTS USING PIV

2.1 Mechanism of Particle Image Velocimetry

Particle image velocimetry (PIV), which is an image analysis method used in this experiment, is a fluid measurement method that can obtain instantaneous velocity of multiple points in a flow field without contact, using two temporally continuous images, the luminance distribution in a minute area in the first time image and the luminance in the area in the second time image. The fluid displacement is calculated by finding the similarity of the pattern and estimating the displacement that is the maximum value as the average displacement vector in the inspection area. The similarity between the luminance patterns of the image at $t = t$ and the image at $t = t + \Delta t$ is calculated by the following equation ;

$$R(\xi, \eta) = \frac{\sum_0^{M-1} \sum_0^{N-1} \{f(m,n) - f_{av}\} \{g(m+\xi, n+\eta) - g_{av}\}}{\sqrt{\sum_0^{M-1} \sum_0^{N-1} \{f(m,n) - f_{av}\}^2} \sqrt{\sum_0^{M-1} \sum_0^{N-1} \{g(m+\xi, n+\eta) - g_{av}\}^2}} \quad (1)$$

where $f(m, n)$ and $g(m, n)$ represent the intensity distribution at time $t = t$ and $t = t + \Delta t$, M and N are the tracking mesh size, ξ and η are the mesh movement amount.

In which

$$f_{av} = \frac{\sum_0^{M-1} \sum_0^{N-1} f(m,n)}{MN} \quad (2)$$

$$g_{av} = \frac{\sum_0^{M-1} \sum_0^{N-1} g(m+\xi, n+\eta)}{MN} \quad (3)$$

Equation (2) and (3) are an average value of the luminance inside each tracking meshes.

From the equation, the displacement of the particle group is determined by (ξ, η) where the similarity $R(\xi, \eta)$ is the highest. These operations are applied to all meshes to calculate the inter-image displacement vector of the whole image. Based on the calculated displacement vector, the shape functions are adopted and the strain is determined.

2.2 Deformation tests on ground model with aluminum bar laminate

To conduct deformation tests on the aluminum bar laminate using PIV, sequent pictures of the deforming laminate are taken, with the equipment moving in equal intervals. To make the particle size distribution as equal as that of Toyoura sand, the aluminum bars are blended with radius 1.6 mm and 3.0 mm at a mass ratio of 2:1. Moreover, to give a wide luminance distribution on PIV analysis, a side of the aluminum bars is multi-colored. Pictures are taken from the side of the aluminum bar laminate in each deformation intervals, and deformation analysis based on PIV is conducted.

In the analysis, analysis mesh is set on the deformation target. The mesh size is 5 mm (to give the luminance variation within the mesh squares).

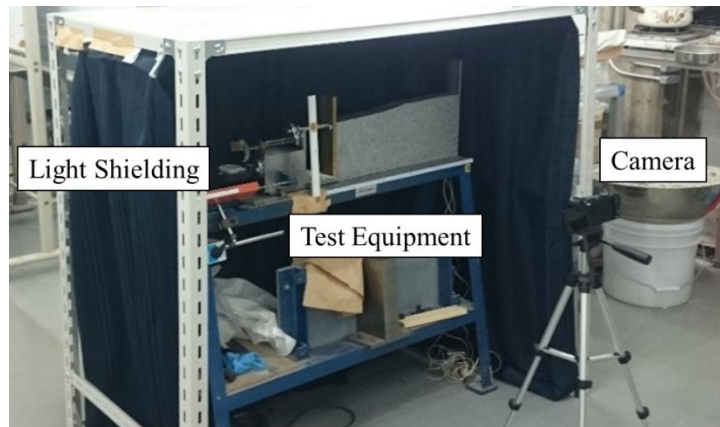


Figure 1: Viewing of deformation test condition

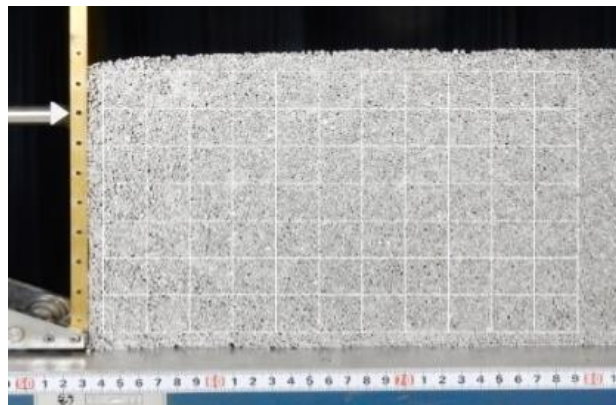


Figure 2: Example of analysis mesh arrangement

2.3.1 Deformation tests on retaining wall movement

The retaining wall test equipment consists of retaining wall and aluminum bar laminated ground that simulates the ground behind the retaining wall. The retaining wall is made by a brass rigid material with a height of 200 (mm), a width of 10 (mm) and a depth of 50 (mm), which can be controlled by the handle to a horizontal displacement of 95 (mm) in active earth pressure direction.

The equipment of the wall model is shown in Figure.3, and the dimensions of the retaining wall test equipment are as shown in Table 1. The ground is tightly packed, and aluminum bars are laid as densely as possible. The test is done with running the wall parallel to the active earth pressure direction. The velocity of wall is set as the deformation is regarded as quasi-static state. The experimental procedure follows as configuration conditions described in Table 2. To avoid the image error due to the setting of camera, filming is done with manual mode, and configurations are shown in Table 3. From the captured pictures, PIV analysis is conducted and confirming the deformation of laminated ground.

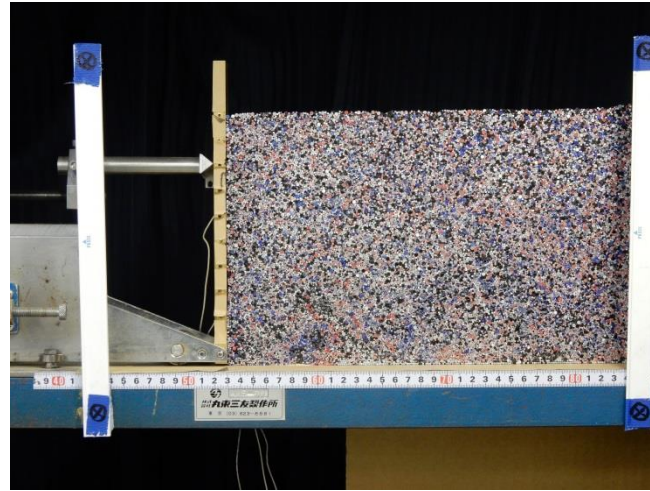


Figure 3: Arrangement of retaining wall test equipment

Table 1: Dimensions of ground model (retaining wall test)

Height (mm)	Depth (mm)	Width(Wall) (mm)	Width(laminate) (mm)
200	50	10	400

Table 2: Configuration of model test (retaining wall test)

Maximum displacement (mm)	Wall movement speed (mm/min)	Filming interval (sec)
60	2	30

Table 3: Configuration of filming condition (retaining wall test)

Pixels	ISO sensitivity	Camera Height	Distance Camera-Model	Shutter speed	Diaphragm value
4608×3456	125	855	1370	1/8	F5.3

2.3.2 PIV analysis results (retaining wall test)

PIV analysis is conducted under the conditions described above, and selection of maximum shear strain contour distribution, which displacements are 10mm and 60mm, is shown in Figure 4. Experimental results are shown with fixed contour, which range is set as 0 to 0.25.

As shown in Figure 4, strain due to the wall movement is clearly captured consistently. It is obvious that there is local large deformation at the bottom of the wall and the contact of slip line and ground surface. The deformation analysis results, which use target markers, are also shown in Figure 5.

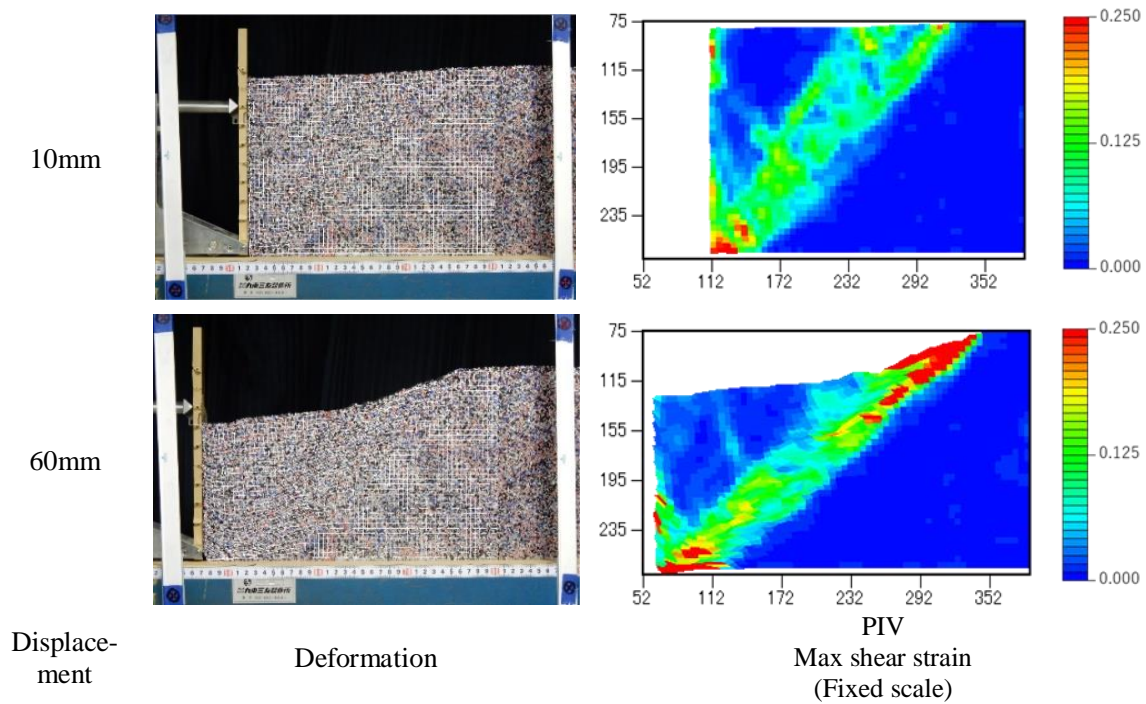


Figure 4 : Results of deformation analysis on retaining wall test using PIV (Selection)

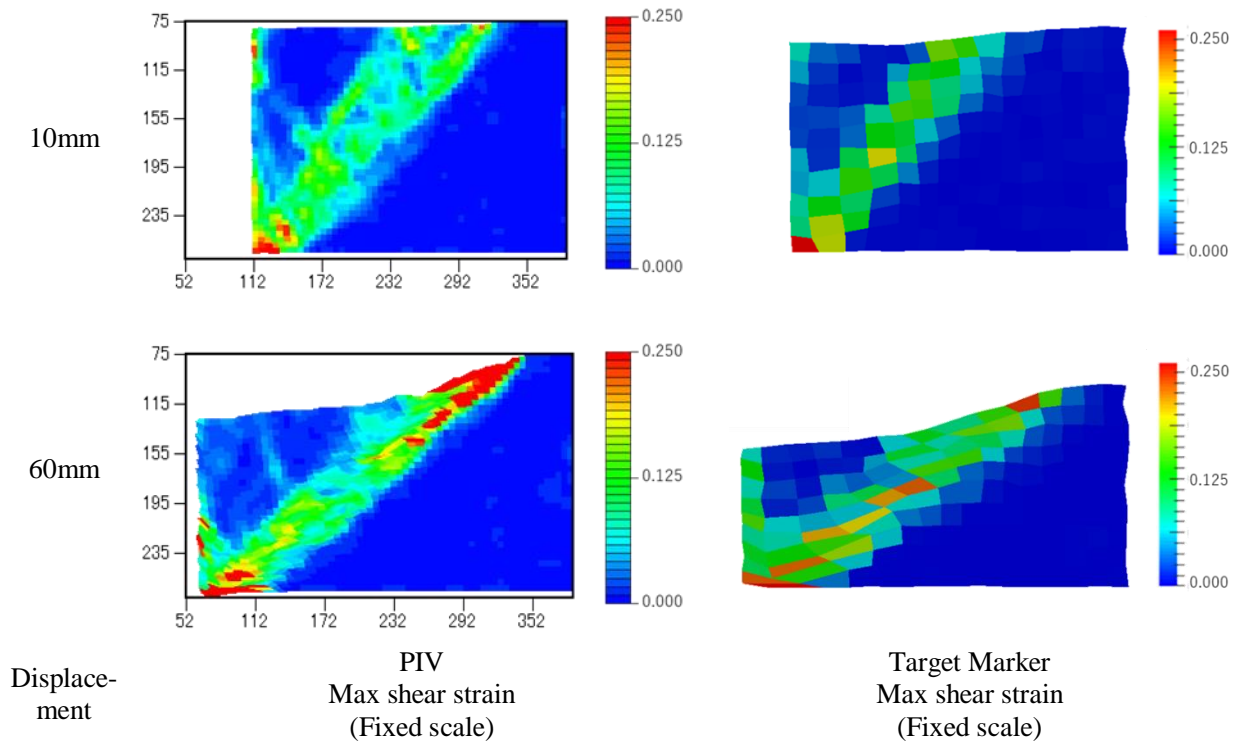


Figure 5 : comparisons of results of deformation analysis (Target marker / PIV)

2.4.1 Deformation tests on shallow foundation loading

The loading test equipment consists of foundation and aluminum bar laminated ground that simulates the ground under the foundation. The foundation is made by a brass rigid material with a height of 60 (mm), a width of 80 (mm) and a depth of 50 (mm), which can be controlled by the handle to a vertical displacement of 30 (mm) from the top of the ground surface. Through experiment, the loading pressure is also measured simultaneously, and obtains a relationship of loading versus displacement.

The equipment of the wall model is shown in Figure.6, and the dimensions of the foundation loading test equipment are as shown in Table 4. The ground is tightly packed, and aluminum bars are laid as densely as possible. The experimental procedure follows as configuration conditions described in Table 5. Filming configurations are also shown in Table 6.



Figure 6 : Arrangement of shallow foundation loading test equipment

Table 4: Dimensions of ground model (foundation loading test)

Height (mm)	Depth (mm)	Width(laminate) (mm)
200	50	523

Table 5: Configuration of model test (foundation loading test)

Maximum displacement (mm)	Foundation loading speed (mm/min)	Filming interval (sec)
25	1	30

Table 3: Configuration of filming condition (foundation loading test)

Pixels	ISO sensitivity	Camera Height	Distance Camera-Model	Shutter speed	Diaphragm value
6000×4000	200	830	1350	1/8	F8.0

2.4.2 PIV analysis results (shallow foundation loading test)

PIV analysis is conducted under the conditions described above, and selection of maximum shear strain contour distribution, in which foundation displacements are 5mm and 22mm, is shown in Figure 7. Experimental results are shown with fixed contour, which range is set as 0 to 0.15. The relationship between loading pressure and displacement of foundation is also shown in Figure 8.

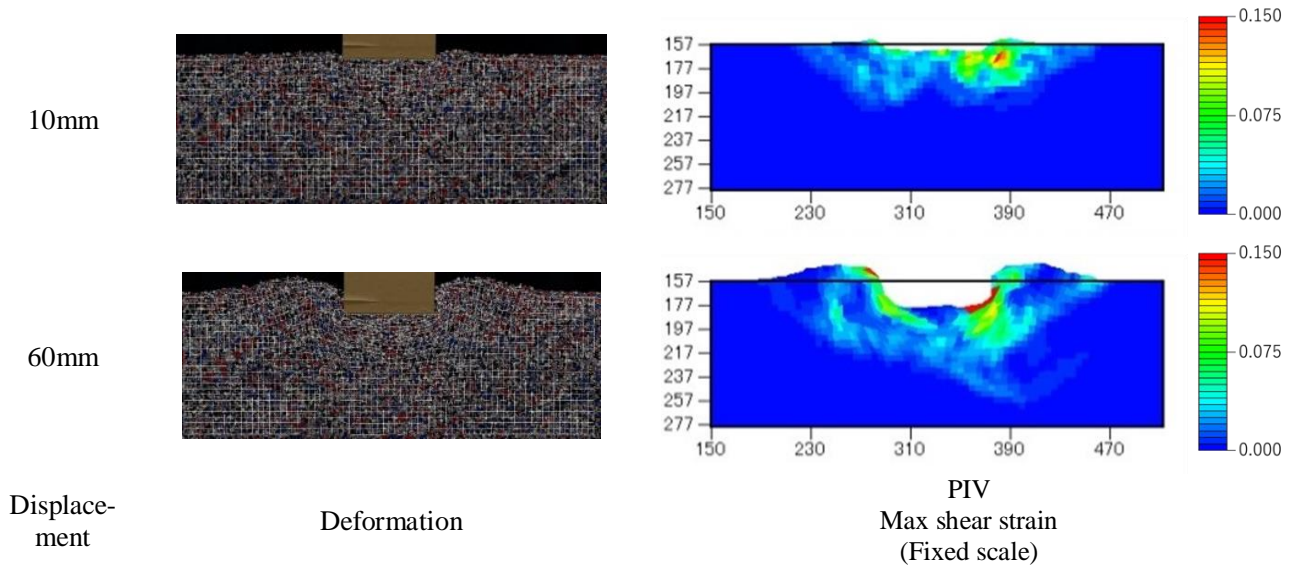


Figure 7: Results of deformation analysis on foundation loading test using PIV (Selection)

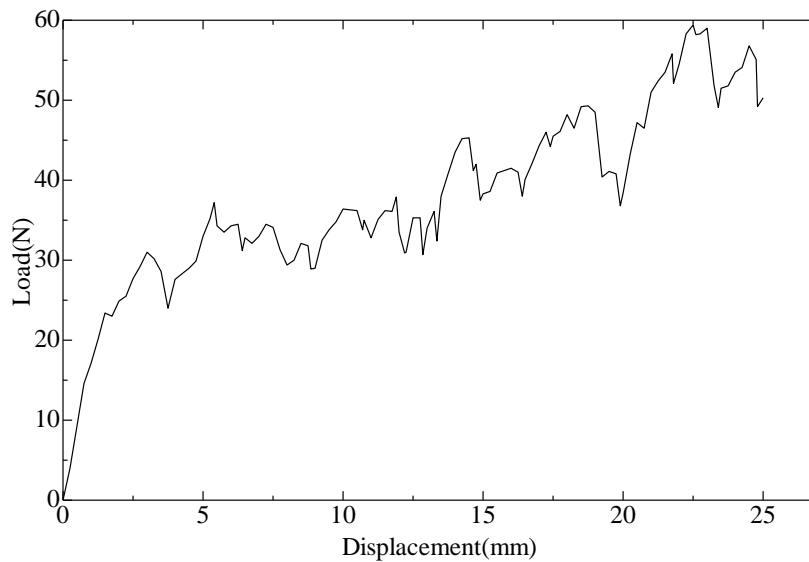


Figure 8: chart of loading versus displacement in foundation test

2.5 Discussions

The higher-resolution deformation tracking in PIV is used as opposed to target markers (Figure 5) since slip surfaces (at 10 mm displacement) are not visible in the latter method. This phenomenon is due to the continuous failure and deformation. Furthermore, the contour range in PIV is higher than that of target marker; strain localization is more clear and easier to capture (Figure 9).

In the foundation loading test, the deformation shape resembles the rupture curve based on Prandtl's theory (Figure 10). However, according to the superposition of PIV results and theoretical curve, the foundation width that matches the captured deformation is smaller than the one derived from Prandtl's theory. As the stress distribution under the foundation is not uniform, it is assumed that the aluminum laminate deforms locally at the edge of foundation. Figure 8 shows the plastic state during the displacement 0-5 mm, and load stress gradually rises with minor fluctuation during the displacement 5-25 mm). Focusing on the minor fluctuation of load with comparing PIV results and chart of loading versus displacement, the deformation spread while loading decreases. As shown in Figure 11, the distribution of the value of the maximum shear strain exceeding 0.075 is increased as the whole ground as compared with the region (a).

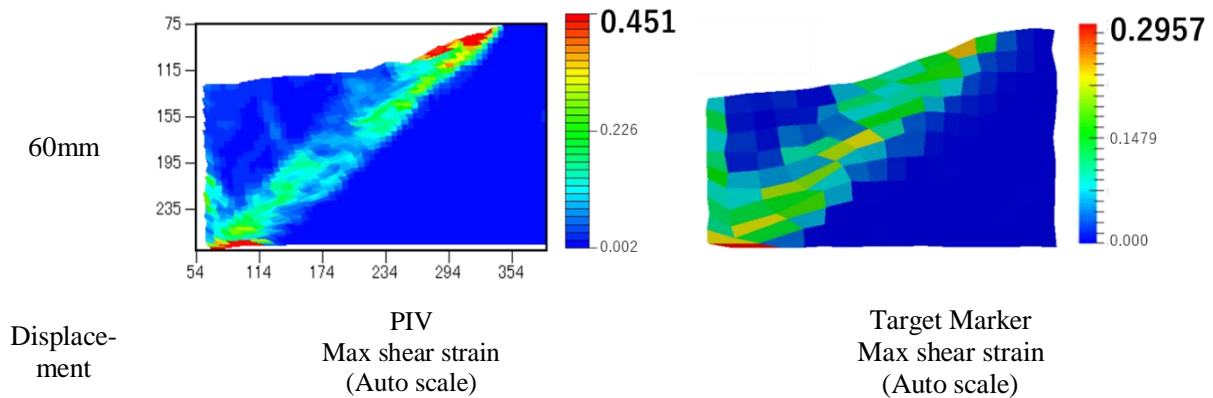


Figure 9: difference of contour range (PIV / target marker) [From Figure. 5]

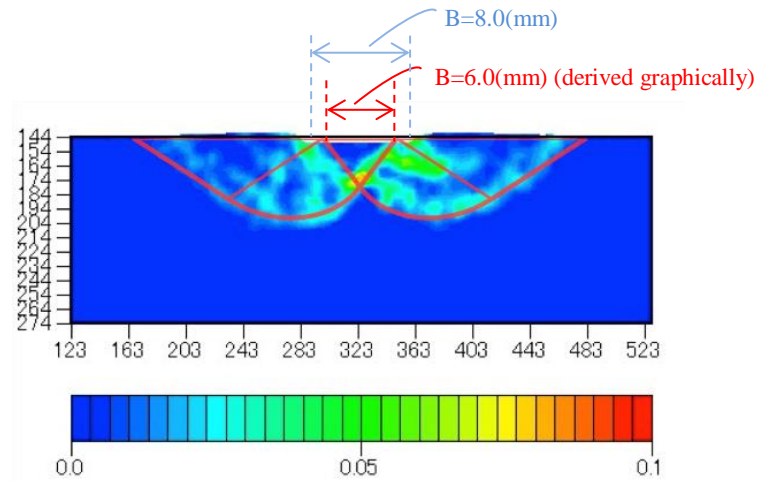


Figure 10: Superposition of PIV result ($d=3.5\sim 4.0\text{mm}$) and Prandtl mechanism

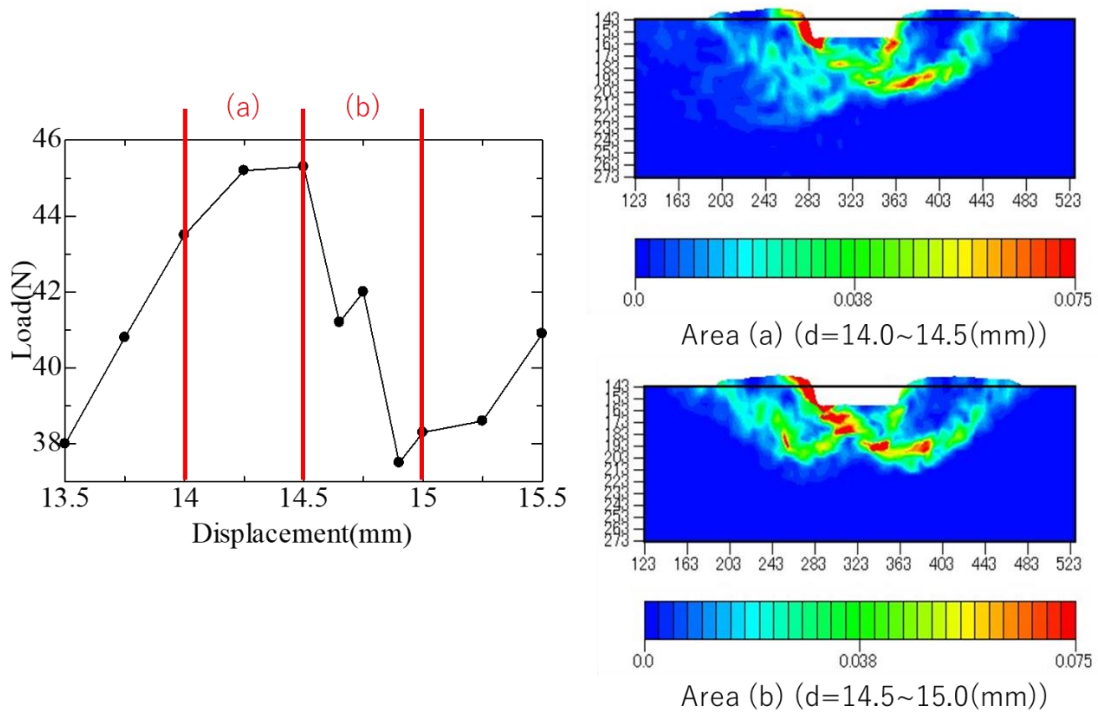


Figure 11: Example of comparison of PIV results and chart of loading versus displacement

5 CONCLUSION

In this paper, the experiments (retaining wall test and foundation loading test) were conducted that to observe ground deformation. This study demonstrates that the PIV analysis captures the deformation more accurately than target markers. Furthermore, evaluating the deformation and experimental values such as loading stress, experimental value is also reexamined based on the PIV analysis results. Therefore, it is shown that detailed phenomenon in ground model can be grasped by utilizing PIV method.

The main finding of this study was that utilizing the PIV method shown above, the criteria for validity of any numerical deformation analysis are confirmed. Large deformation, such has not been explained in formula, is reproduced in numerical analysis, therefore the experimental deformation results are needed. Thus the aforementioned method is more efficient and numerical analysis can be properly evaluated.

REFERENCES

- [1] DJ White, WA Take and MD Bolton, Soil deformation measurement using particle image velocimetry (PIV) and photogrammetry, *Geotechnique* 53, No. 7, 619–631, 2003
- [2] Prandtl, L.: “On the penetrating strength (hardness) of a plastic construction materials and the strength of cutting edges”, *Zeit. angew. Math. Mech.*, 1. No.1,1921
- [3] T. Miura, H. Akagi and T. Kiriya (2016). Experimental study on large deformation behaviors of the ground behind retaining walls, The 71st Japan Society of Civil Engineers Conference, 177-178 (in Japanese).
- [4] S. Sreng and K. Ueno (2004). Deformation behavior and bearing capacity of sand under two adjacent foundations, *Japan Society of Civil Engineers*, Vol.7, 65-74 (in Japanese)
- [5] R.F. Scott : *Principles of Soil Mechanics*, Appendix B, 1965